

Supporting Information

Humphrey et al. 10.1073/pnas.1318176111

SI Methods

Site Description and Dating. The Iberomaurusian refers to a Later Stone Age industry characterized by microlithic backed bladelets and to the people who produced this industry, and is recorded at numerous sites from inland and coastal areas of the Maghreb (1). A key Iberomaurusian site is Grotte des Pigeons at Taforalt, which is located in the Beni-Snassen Mountains at an elevation of 720 m above sea level, near the border between Morocco and Algeria (34°48'38" N, 2°24'30" W). The enormous potential of the site came to light during excavations by Jean Roche (2). Roche described a number of stratigraphic layers containing Iberomaurusian, the upper ones being gray ashy (*couches cendreuses*) and the underlying ones clayey sand (*couches argilo-sableuses*) deposits (2). Excavations in 1954–1955 uncovered an extensive series of Iberomaurusian human burials in gray ashy deposits situated toward the back of the cave (2).

New work on the Iberomaurusian sequence at Taforalt was conducted between 2003 and 2013 (3, 4). Excavation trenches were located alongside the sections dug by Roche on the south side of the cave (Sector 8) (Fig. 1) and in a recess at the back of the cave (Sector 10) (Fig. 1). The Iberomaurusian sedimentary sequence for Sector 8 is 4.8 m deep and is shown in schematic form (Fig. S1). Within the sequence there is a major stratigraphic division between the Grey Series (Roche's ashy deposits) and an underlying Yellow Series (his clayey sands). The Grey Series are essentially anthropogenic sediments, originally more than 4 m thick and spread over an area in excess of 800 m². No human burials or other human remains were recovered in Sector 8.

The Iberomaurusian part of the Sector 8 sequence (Grey and upper Yellow Series) has been dated by radiocarbon accelerator mass spectrometry (AMS) using ultrafiltration (5), producing dates on bone and wood charcoal that span the period 20.5–12.6 ka (4). All of the dates lie within the range of the IntCal09 calibration curve (6, 7). The authors provide an earliest calibrated age for the Grey Series of 15,204–14,261 cal B.P. No clear stratigraphic subdivisions were discernible in Sector 10, which is made up of very loose ashy sediments. Burials in Sector 10 were situated within a recess at the back of the cave in an area of restricted height (Fig. 1). Seven human bone samples representing six individuals have been directly dated by AMS using ultrafiltration (Table S1). All samples had good collagen preservation (>2% collagen by weight), carbon content (41–47%), and CN ratio (3.1–3.2), but one sample, bone 4797 (OxA-16663), was very small (starting weight 100 mg) and consequently has a higher SE. The ages have been calibrated by OxCal 4.1 and occur within the same age range as the base of the Grey Series in Sector 8.

Dental and Skeletal Observations. The skeletal sample derives from the Iberomaurusian necropolis excavated by Roche in 1954 and 1955 (2) and recently excavated burials from Sector 10 (3). Preservation was variable, with some individuals represented by complete skeletons, and others only by fragmentary dental remains. In total, 52 individuals were represented by at least a fragment of the upper or lower jaw. All teeth and alveoli were observed in the sample, giving a total of 941 observable sockets.

Age Estimation. Where possible, age estimation was carried out using pubic symphysis morphology, auricular surface morphology, ectocranial suture closure, and sternal rib end changes (8). Based on these observations, the sample was divided into three age

categories: young adult ($n = 6$), middle adult ($n = 16$), old adult ($n = 3$), and an undetermined category ($n = 27$).

Dento-Alveolar Parameters. A series of dento-alveolar parameters were recorded by I.D.G. The number of observations for each of these parameters depends on the presence and preservation of teeth and alveoli (tooth sockets). Observed sockets are defined as observable sockets minus sockets affected by postmortem tooth loss (PMTL). Observed teeth are the observable sockets minus sockets affected by postmortem and antemortem tooth loss (AMTL). All teeth were examined with good lighting and a magnification of 4× and 10×. The comprehensive data collection protocol of Hillson (9) was followed and each tooth site scored. For this study, data are summarized into broader categories.

Tooth Wear. Tooth wear was recorded using the Smith system (10) for incisors, canines, and premolars, and the Scott system for occlusal wear in molars (11). Left and right sides are not considered independently and the highest value was used if both sides were present. Tooth wear in upper and lower dentitions has been noted to vary (9), so upper and lower tooth wear rates are considered separately. Mean tooth wear for each observed tooth was calculated for all individuals in the sample. Tooth wear is reported for the whole sample and for subsamples of young adults, middle adults, and old adults (Table S2).

Tooth Loss. PMTL was defined as an empty socket showing no sign of alveolar remodeling (12). PMTL is reported as a proportion of observable sockets. AMTL was defined as an empty socket showing any sign of alveolar remodeling (12). Because of the high prevalence of evulsion of the upper central incisors in the Taforalt sample, we report AMTL as both total AMTL and postcanine AMTL. In both cases, AMTL is reported as a proportion of observed sockets.

Alveolar Bone Resorption (Root Exposure). Alveolar bone resorption was recorded as present if a distance of at least 2 mm was measured between the crest of the alveolar bone and the cemento-enamel junction on any surface of the tooth crown (mesial, distal, lingual, or buccal). Root exposure is reported as a proportion of observed teeth.

Abscesses. Abscesses were recorded by direct observation only and defined as a periapical cavity in the alveolar bone, with relatively smooth walls. Abscesses are reported as a proportion of observable sockets.

Caries Diagnosis. Caries were recorded using Hillson's categories (9). All tooth surfaces were observed for carious lesions. Caries were recorded for the following crown locations: (i) occlusal molar fissures, (ii) occlusal attrition caries in the dentine, (iii) buccal surface, (iv) lingual surface, (v) mesial surface, (vi) distal surface, (vii) pit caries, and (viii) rim chipping caries. Crown caries refer to the presence of caries on one of more of these locations. A carious lesion was considered present when there was clear penetration in the enamel (score 3 or above). Root surface caries describe lesions affecting any dentine surface below the enamel dentine junction. Gross caries was used when a lesion affected more than one location and its origin could no longer be determined (score 7 or 8). Caries prevalence is expressed as the proportion of carious teeth.

Macrobotanical Observations. Macrobotanical remains, excluding wood charcoals, were examined by J.M. in soil samples from a number of closely spaced columns in Sector 8 (Fig. S1). Samples collected in 2003 comprise three continuous sequences, each located slightly deeper into the cave than the one above. The 2003 samples are numbered (Fig. S1, from top) G88 to G96.3, G96.4 to G96.5 (G96.6 was not sampled), and G97 to G99. Sample G100 and the underlying samples from units Y1 to upper Y4 were collected in 2004–2005. These samples are in stratigraphic order but not in a continuous sequence and were located slightly toward the rear of the cave. Samples collected in 2009–2010 are from a continuous sequence from 10 to 475-cm depth and are numbered MMC 1–54 and MMC 80–130 (there was no actual gap between sample 54 and sample 80). These columns can be cross referenced to a central excavation column with Grey Series layers L1–L29 and Yellow Series layers Y1–Y4. The stratigraphic links between all these columns are shown schematically in Fig. S1; the real lateral distance between the G series (left-outermost) and MCC series (right-innermost) is ~5 m.

Macrobotanical remains were collected by floating each soil sample and then sieving the flot (light fraction) using a column of sieves with a mesh size of 4, 2, 1, and 0.5 mm. A total of 100 samples were analyzed, with a total volume of 349.9 L. The coarse stone fraction was removed from the soil samples on site and is excluded from volume measurements. Density of remains was high, averaging about 3.63 items per liter. In total, 1,273 macrobotanical items were collected. Density of macrobotanical remains is higher in the Grey Series samples than in samples from the Yellow Series, even though the Grey Series samples contain

more fine stones than samples from the slower accumulating Yellow Series.

All plant remains are carbonized and very well preserved (Fig. S2). The plant fossils were identified using a binocular microscope (8–80× magnification) and the reference collections of the Department of Historical Sciences, University of Las Palmas de Gran Canaria (Spain) and the McDonald Institute for Archaeological Research, University of Cambridge. Identification to species level was attempted for key taxa. Identification of oak species based on seeds is difficult as there are several species growing in the region that produce edible acorns with a similar shape and size. Identification to species level was only possible if the scales in the cupules were well preserved. Scales in the remains from Taforalt are short, ovate, glabrescent, and apressed (Fig. 3), and these are diagnostic features of *Quercus ilex* (13). Although these data suggest that acorns from the Holm Oak were the focus of gathering, it is possible that other oak species present in the region were also exploited. In the case of pine cones, the scales have a prominent and pyramidal apophysis, a diagnostic feature that enabled identification as *Pinus pinaster* (13). Oak and pine remains occur throughout the Grey Series but only one fragment of oak and none of pine was identified in the Yellow Series samples. The number and range of plant species recorded in the Grey Series is similar in the soil samples collected in 2003–2005 and those collected in 2009–2010 (Table 2). Proportions of different taxa are similar throughout the Grey Series, suggesting that the plant assemblage is homogeneous. Information on ripening times and nutritional value of key plant taxa was assembled from published sources (Table S3).

- Irish JD (2000) The Iberomaurusian enigma: North African progenitor or dead end? *J Hum Evol* 39(4):393–410.
- Roche J (1963) *L'Épipaléolithique Marocain* [The Moroccan Epipalaeolithic] (Livraria Bertrand, Portugal). French.
- Humphrey L, Bello SM, Turner E, Bouzouggar A, Barton N (2012) Iberomaurusian funerary behaviour: evidence from Grotte des Pigeons, Taforalt, Morocco. *J Hum Evol* 62(2):261–273.
- Barton RNE, et al. (2013) Origins of the Iberomaurusian in NW Africa: New AMS radiocarbon dating of the Middle and Later Stone Age deposits at Taforalt Cave, Morocco. *J Hum Evol* 65(3):266–281.
- Brock F, Higham T, Ditchfield P, Ramsey CB (2010) Current pretreatment methods for AMS radiocarbon dating at the Oxford Radiocarbon Accelerator Unit (ORAU). *Radiocarbon* 52(1):103–112.
- Reimer PJ, et al. (2009) IntCal09 and Marine09 radiocarbon age calibration curves, 0–50,000 years cal BP. *Radiocarbon* 51(4):1111–1150.
- Ramsey CB (2009) Bayesian analysis of radiocarbon dates. *Radiocarbon* 51(1):337–360.
- Buikstra JE, Ubelaker DH (1994) *Standards for Data Collection from Human Skeletal Remains: Proceedings of a Seminar at the Field Museum of Natural History* (Arkansas Archaeological Survey Press, Fayetteville).
- Hillson S (2001) Recording dental caries in archaeological human remains. *Int J Osteoarchaeol* 11(4):249–289.
- Smith BH (1984) Patterns of molar wear in hunger-gatherers and agriculturalists. *Am J Phys Anthropol* 63(1):39–56.
- Scott EC (1979) Dental wear scoring technique. *Am J Phys Anthropol* 51(3):213–217.
- Ortner DJ, Putschar W (1981) *Identification of Pathological Conditions in Human Skeletal Remains* (Smithsonian Institution, Washington, DC).
- Fennane M, et al. (1999) *Flore Pratique du Maroc, volumen 1. [Useful Flora of Morocco, volume 1]* (Institut Scientifique, Rabat), French.

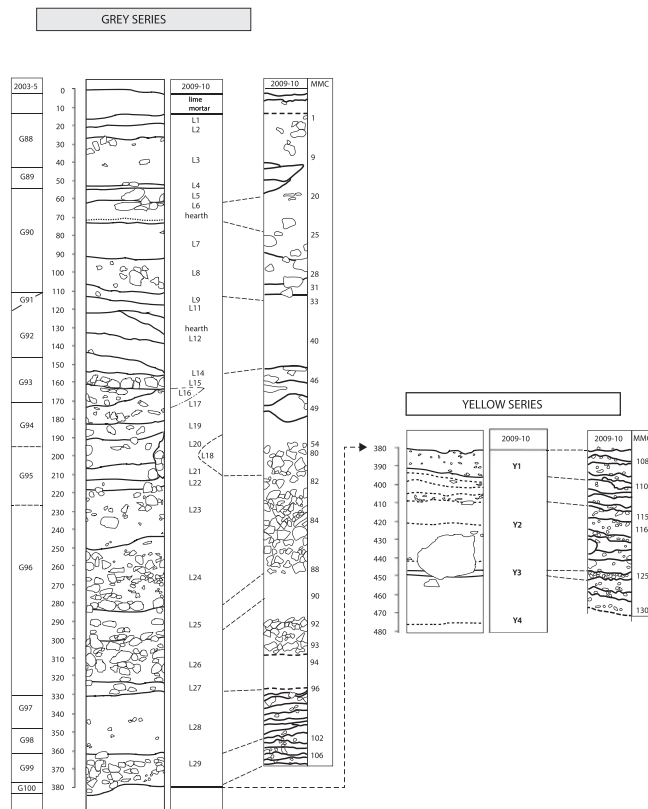


Fig. S1. Schematic section through the Iberomaurusian Grey and Yellow Series deposits in Sector 8, with the units sampled for macrobotanical analysis.

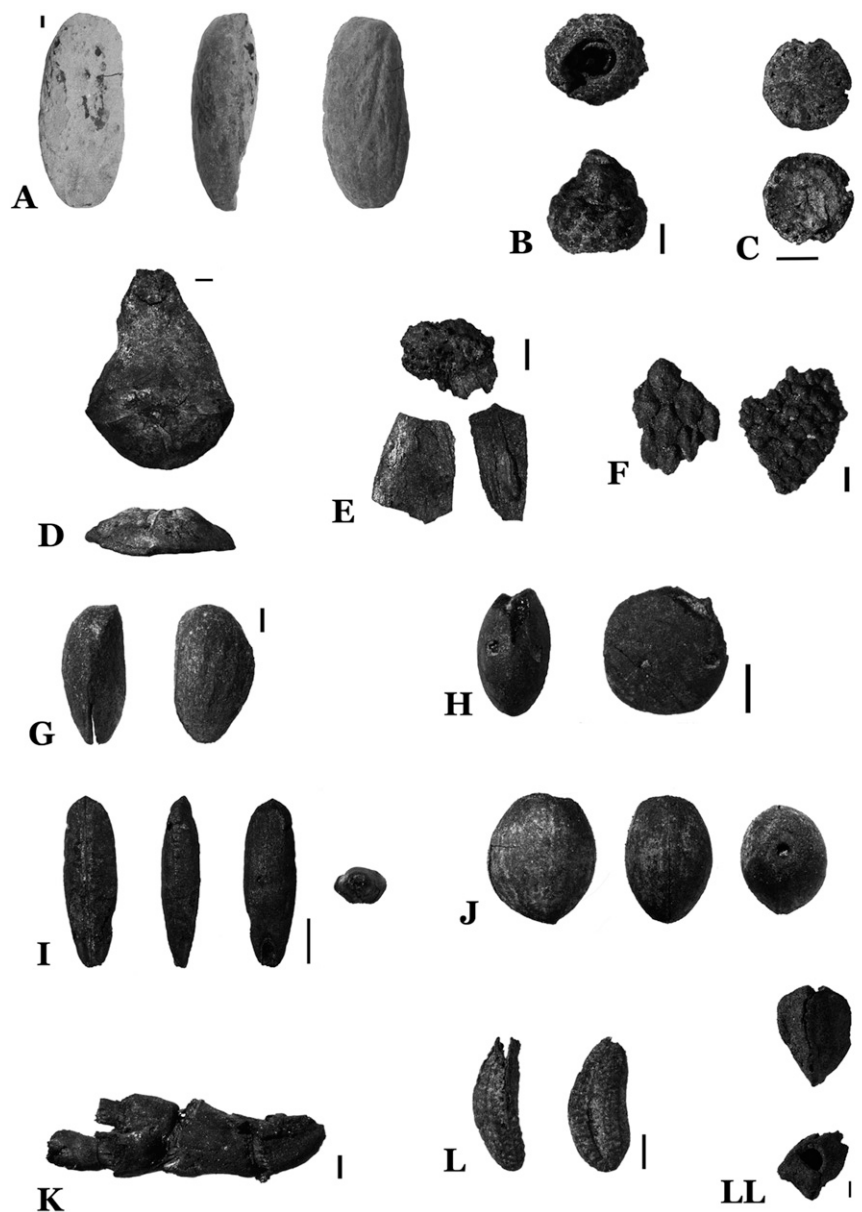


Fig. S2. Macrobotanical remains from Taforalt (scale, 1 mm): (A) *Quercus* sp., cotyledon; (B) *Quercus ilex*, immature cupule; (C) *Quercus* sp. abscission scar; (D) *Pinus pinaster*, seed scale; (E) *Quercus* sp. pericarp and pericarp still attached to the abscission scar; (F) *Quercus ilex*, scales of the cupule; (G) *Pinus pinaster*, seed; (H) *Lens* cf. *nigricans*, seed; (I) *Avena* sp., seed; (J) *Pistacia terebinthus*, seed; (K) *Stipa tenacissima*, rhizome fragment; (L) *Sambucus nigralebula*, seed; (LL) *Juniperus phoenicea*, seed.

Table S1. Radiocarbon determinations and calibrated ages (IntCal09) of human bone from Sector 10

Sample	Specimen	Layer	¹⁴ C determination	Calibrated (B.P.) 95.4%
OxA-16663	Infant humerus	Undisturbed primary burial	12470 ± 100	15077–14132
OxA-23660	Adult vertebra	Disturbed context	12380 ± 55	14930–14076
OxA-23778	Adolescent metatarsal	Undisturbed primary burial	12265 ± 50	14824–13920
OxA-23779	Infant humerus	Undisturbed primary burial	12255 ± 50	14805–13908
OxA-23780	Infant clavicle	Undisturbed primary burial	12355 ± 50	14890–14049
OxA-23781	Adult femur	Disturbed primary burial	12410 ± 50	14956–14120
OxA-23782	Adult femur (repeat)	Disturbed primary burial	12460 ± 55	15016–14163

Table S2. Mean tooth wear stages for upper and lower dentition

Upper or lower dentition	Age				Total
	Young adult	Middle adult	Old adult	Undetermined	
Upper					
M3	3	4	9	4	5
M2	5	6	5	6	6
M1	6	8	5	8	7
C	4	5	8	5	6
P4	4	6	8	5	6
P3	4	6	8	5	6
I2	4	5	8	5	5
I1	2	4		2	2
Lower					
M3	3	4	8	5	5
M2	4	6	9	6	6
M1	5	8	10	7	7
C	3	6	7	5	5
P4	3	6	7	5	5
P3	4	5	6	5	5
I2	3	5	4	5	4
I1	3	4	4	4	4

Table S3. Nutritional value and ripening season of the most abundant edible plants identified in Taforalt

Species	Common name	Nutritional value (g/100 g)			Ripening season
		Carbohydrates	Lipids	Protein	
<i>Quercus ilex</i> L. (1)	Acorn	53.0	10.5	3.0	Autumn
<i>Pinus pinaster</i> Aiton (1)*	Pine nut	5.0	51.1	33.2	Autumn
<i>Juniperus phoenicea</i> L. (2)	Juniper	18.0	4.0	5.0	Autumn
<i>Pistacia terebinthus</i> L. (2)	Terebinth pistachio	5.0	61.0	4.0	Autumn
<i>Lens cf. nigricans</i> , <i>Lathyrus</i> sp., <i>Vicia</i> sp. (3) [†]	Wild pulse	58.0	2.0	26.0	Summer
<i>Avena</i> sp. (4)	Wild oat	55.0	8.0	20.0	Summer
<i>Sambucus nigra/ebulus</i> (3)	Elderberry	55.0	1.0	7.0	Autumn
<i>Triticum</i> sp. (5)	Wheat	71.1	2.5	13.6	

Data for wheat provided as comparison.

*Data for *Pinus pinea* L.

[†]Data for *Lens culinaris* Medik.

- Gonçalves Ferreira FA, da Silva Graça ME (1963) *Tabela da Composição dos Alimentos Portugueses [Table of Compositions of Portuguese Foods]*. (Report for Ministerio da Saude e Assistencia, Direção Geral de Saude, Lisboa). Portuguese.
- Debussche M, Cortez J, Rimbault I (1987) Variation in fleshy fruit composition in the Mediterranean region: The importance of ripening season, life-form, fruit type and geographical distribution. *Oikos* 49(3):244–252.
- Urbano G, Porres JM, Frias J, Vidal-Valverde JC (2009) *Lentil: An Ancient Crop for Modern Times*, eds Yadav SS, McNeil DL, Stevenson PC (Springer, Heidelberg), pp 47–93.
- Sosulski FW (1985) Processing and composition of wild oat groats (*Avena fatua* L.). *J Food Eng* 4(3):189–203.
- QA international Collectif (2012) *The Visual Food Encyclopedia* (Québec Amérique, Quebec).